

Winter mesoscale variations of carbonate system parameters and estimates of CO₂ fluxes in the Gulf of Cadiz, northeast Atlantic Ocean (February 1998)

Melchor González-Dávila and J. Magdalena Santana-Casiano

Chemistry Department, Las Palmas de Gran Canaria University, Las Palmas, Gran Canaria, Spain

Evgeny V. Dafner

Department of Oceanography, School of Ocean, Earth Sciences and Technology, University of Hawaii, Manoa, Honolulu, Hawaii, USA

Received 4 December 2001; revised 12 June 2003; accepted 12 September 2003; published 8 November 2003.

[1] Further observations with small spatial and temporal resolutions conducted during different seasons are required in order fully to understand the role that shelves play in the global carbon cycle. The components of the carbonate system (total alkalinity, pH in the total scale, total dissolved inorganic carbon, and CO₂ fugacity), and dissolved oxygen, nutrients, and phytopigments were studied along the mesoscale section over the continental shelf and slope in the Gulf of Cadiz in February 1998. All the chemical properties clearly distinguish four different water masses: Gulf of Cadiz Water, North Atlantic Surface Water, North Atlantic Central Water, and Mediterranean Water. From the thermohaline properties and applied chemical conservative tracers for each water mass, a mixing model has been established which explains more than 96% of the variability in the distribution of chemical properties. The relative variation of nutrients and carbon concentrations resulting from the regeneration of organic matter was estimated. The contribution of Mediterranean water to the waters at the traverse of Cadiz varies from 15% to 40% according to this model. The difference of $f\text{CO}_2$ between seawater and atmosphere ($\Delta f\text{CO}_2 = -35 \mu\text{atm}$) shows that the surface seawater in the Gulf of Cadiz is a sink for atmospheric CO₂ during winter with an average calculated net CO₂ flux across the air-sea interface of about $-19.5 \pm 3.5 \text{ mmol m}^{-2} \text{ d}^{-1}$. We estimate that at the traverse of Cadiz the shallow core of Mediterranean outflow carries out $1.2 \bullet 10^4$ to $2.4 \bullet 10^4 \text{ mol inorganic carbon s}^{-1}$. This estimate is 1 order of magnitude lower than that calculated for the Mediterranean outflow in the Strait of Gibraltar.

INDEX TERMS: 4806 Oceanography: Biological and Chemical: Carbon cycling; 4271 Oceanography: General: Physical and chemical properties of seawater; 4805 Oceanography: Biological and Chemical: Biogeochemical cycles (1615); 4219 Oceanography: General: Continental shelf processes; **KEYWORDS:** carbon dioxide, flux, Gulf of Cadiz

Citation: González-Dávila, M., J. Magdalena Santana-Casiano, and E. V. Dafner, Winter mesoscale variations of carbonate system parameters and estimates of CO₂ fluxes in the Gulf of Cadiz, northeast Atlantic Ocean (February 1998), *J. Geophys. Res.*, 108(C11), 3344, doi:10.1029/2001JC001243, 2003.

1. Introduction

[2] It has long been recognized that the oceans are an intense sink of carbon dioxide in the global carbon cycle which absorbs about 30–40% of the carbon of anthropogenic origin released into the atmosphere [Siegenthaler and Sarmiento, 1993]. However, little is yet known about the role that continental shelves play in the carbon cycle (i.e., whether shelves act as a sink or source of carbon dioxide). In the open ocean, air-sea exchange of CO₂ is driven by the warming and cooling of surface waters, wax and wane of plankton blooms, wind velocity, lateral advection and upwelling [Bakker *et al.*, 1997]. In the shelf, the same

processes occur but on a smaller spatiotemporal scale, and with greater intensity and variability, affected by river discharge and tidal forcing. In addition, the carbon cycle in coastal areas is also affected by exchanges with bottom sediments and by large variations in the land atmospheric CO₂ as a function of wind direction [Bakker *et al.*, 1996; Schneider *et al.*, 1992]. More observations are needed in both small spatial and temporal resolution conducted in different seasons in order to understand the role that shelves play in the global carbon cycle.

[3] The Gulf of Cadiz shelf is of special interest because it immediately precedes the Strait of Gibraltar. The study of the carbon exchange throughout this strait began only a few years ago and it has already been emphasized that the Gulf of Cadiz plays an important role in the carbon cycle of the

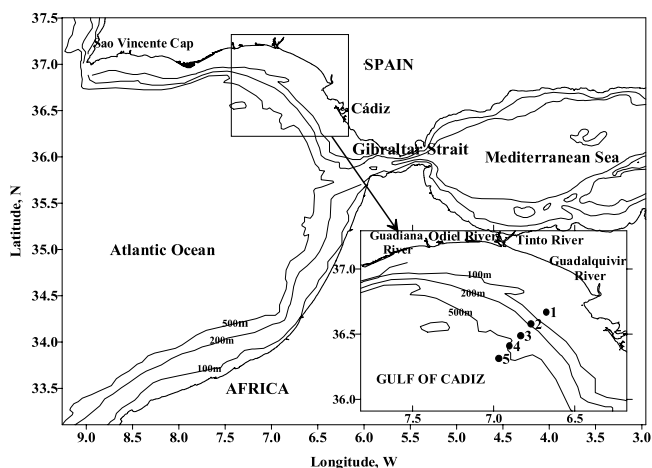


Figure 1. Bathymetry the Gulf of Cadiz and stations grid during the cruise on board the RV *Cornide de Saavedra* (10–11 February 1997).

eastern North Atlantic [Parrilla, 1998] and the Mediterranean Sea [Dafner *et al.*, 2001]. First, in the Gulf of Cadiz there are several water masses mixing to form the “Atlantic inflow” which is responsible for the general oligotrophic and relatively well oxygenated regime of the north-western Mediterranean Sea [Packard *et al.*, 1988; Minas *et al.*, 1991]. Second, this area is on the pathway of the “Mediterranean outflow” which thereafter enters to the open ocean and influences the circulation of the North Atlantic and climate in general [Rahmstorf, 1998].

[4] The Gulf of Cadiz is well documented from a physical point of view [Madelaine, 1967; Zenk, 1975; Ambar *et al.*, 1976; Ochoa and Bray, 1991; Price *et al.*, 1993]. Despite its initially very high density ($\sigma_0 = 28.95 \text{ kg m}^{-3}$), the Mediterranean outflow does not reach the bottom of the open North Atlantic ($\sigma_0 \cong 27.95 \text{ kg m}^{-3}$) because it entrains a substantial volume of the overlying North Atlantic Central water while still in the Gulf of Cadiz. As the outflow exits the strait, it flows across isobaths as a density current, though under the influence of the Earth’s rotation. Two distinct Mediterranean water layers appear in profiles from the open northeast Atlantic [Zenk, 1975]. A separate, shallower layer of the outflow also appears west of about 7°W [Ambar, 1983]. An entrainment of Atlantic water modifies the characteristics as well as the volume of the outflow. Similarly, the inflow is modified by its contact with the outflow, increasing the minimum salinity of the Atlantic water from 35.6 in the Gulf of Cadiz to 36.2 and higher in the strait. However, until now, only a few papers on the biogeochemical processes of this shelf have been presented [Ambar *et al.*, 1976; Cano, 1978; Minas and Minas, 1993; Minas *et al.*, 1991]. The relative contributions of these processes on the carbonate system, however, are still largely uncharted.

[5] In response to increased interest in global carbon change, measurements of the marine carbon system (i.e., CO_2 fugacity, total inorganic carbon, titration alkalinity and pH_t) have been included in the European CANIGO project (Canary Islands Azores Gibraltar Observations, MAST III Programme). This paper is the first attempt to estimate processes governing the carbon cycle on a small spatiotem-

poral scale in the Gulf of Cadiz continental shelf. As the following discussion will show, interaction between different water masses, river discharge, and winter mixing influences on the biogeochemistry of the eastern North Atlantic and Mediterranean Sea make this area a unique site for the understanding of the contribution of the mesoscale variability of inorganic carbon features to the global carbon cycle.

2. Material and Methods

2.1. Sampling Field

[6] Discrete seawater samples were taken from the RV *Cornide de Saavedra* with a CTD rosette system equipped with 10-L Niskin bottles between 10 and 11 February 1998 at five stations along a section in the Gulf of Cadiz (Figure 1). Neil Brown MKIIB CTD was used to obtain continuous profiles of temperature and salinity. The CTD’s pressure and temperature sensors were calibrated in the laboratory to WOCE standards (better 2 mK, 3 dbar at 6000 dbar). The conductivity sensor was calibrated by comparison with the in situ conductivity of bottle samples taken during the up profile with the rosette.

[7] The short distances between the stations (8.6 to 19.1 km or 4.8 to 9.0 nautical miles) together with the fact that the samples were taken within 24 hours, allows us to hypothesize on the mesoscale nature of the properties described here. While tides affect distribution of physical and chemical properties in the water column at the shore stations (stations 1 and 2), our data represents values determined under the sampling conditions. The rationale for site selection at the traverse of Cadiz was (1) to consider a wide and shallow shelf with a depth of under 50 m influenced by the discharge of the Guadalquivir river; and (2) the separation of the Mediterranean outflow in this area into three cores: shallow, upper, and lower [Ambar and Howe, 1979a, 1979b].

2.2. Carbonate System Measurements

[8] The pH_t in total scale (mol (kg-SW)^{-1}) was measured following the spectrophotometric technique of Clayton and Byrne [1993] using the m-cresol purple indicator [Department of Energy, 1994]. Here 0.0047 pH units were added to the pH experimental values in order to take into consideration the recommendations by DelValls and Dickson [1998] and Lee *et al.* [2000]. A system similar to that described by Bellerby *et al.* [1995] was developed in our lab. The pH_t measurements were carried out using a Hewlett Packard Diode Array spectrophotometer in a 25°C -thermostated 1-cm flow-cell using a Peltier system. A stopped-flow protocol was used to analyze seawater previously thermostatted to 25°C for a blank determination at 730, 578, and 434 nm. The flow was restarted, and the indicator injection valve switched on to inject 10 μl dye through a mixing coil (2 m). Three photometric measurements were carried out for each injection in order to remove all dye effect on the seawater pH_t measurement. Repeatedly, seawater measurements of the different Certified Reference Materials (CRM provided by A. G. Dickson, Scripps Institution of Oceanography) samples gave a standard deviation of ± 0.0015 ($n = 54$).

[9] The total alkalinity of seawater (A_T) was determined by titration with HCl to the carbonic acid end point using two similar potentiometric systems, as described in more

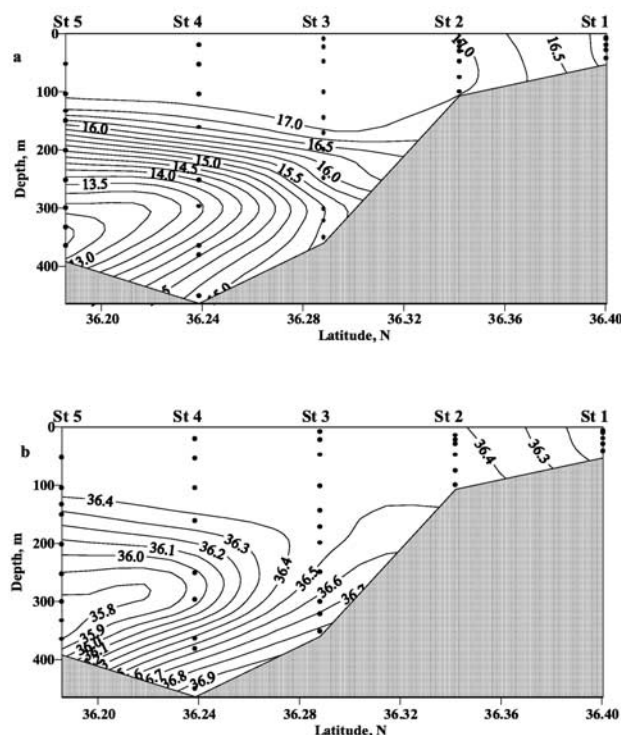


Figure 2. Distribution of (a) temperature ($^{\circ}\text{C}$) and (b) salinity along the section at the traverse of Cadiz (10–11 February 1998, Gulf of Cadiz). Hereinafter the bottom is the depth observed at each station and does not constitute a typical bathymetric profile.

detail by *Mintrop et al.* [2000]. In order to yield an ionic strength similar to open ocean seawater, the HCl solution (25 l, 0.25 M) was made from concentrated analytical grade HCl (Merck[®], Darmstadt, Germany) in 0.45 M NaCl. The acid was standardized by titrating weighed amounts of Na_2CO_3 dissolved in 0.7 M NaCl solutions. The total alkalinity of seawater was evaluated from the proton balance at the alkalinity equivalence point, $\text{pH}_{\text{equiv}} = 4.5$, according to the exact definition of total alkalinity [*Dickson*, 1981]. The performance of the titration systems was monitored by titrating different samples of certified reference material (CRM, batch 42) with known inorganic carbon and A_T values. The agreement between our data and CRM values was within $\pm 1.5 \mu\text{mol kg}^{-1}$.

[10] Total inorganic carbon (C_T) was computed from experimental values of pH_T and total alkalinity, using the carbonic acid dissociation constants of Mehrbach after *Dickson and Millero* [1987]. This set of constants presented the best agreement between $C_T(\text{pH}, A_T)$ calculations and certified C_T values for CRM, batch 42, with a C_T residual of $\pm 3 \mu\text{mol kg}^{-1}$, $n = 54$ [*Millero*, 1995; *Lee et al.*, 1997].

[11] Fugacity of carbon dioxide ($f\text{CO}_2$) in the air and in surface seawater was determined using a flow system similar to the unit designed by *Wanninkhof and Thoning* [1993] and developed by Frank J. Millero's group at the University of Miami. The equilibrator used is based on the design by R.F. Weiss and described by *Butler et al.* [1988]. The concentration of CO_2 in the air and in the equilibrated air sample was measured with a differential, non-dispersive, infrared gas analyzer supplied by LI-COR (LI-6262 CO_2 /

H_2O Analyzer). The sample was measured wet and the signal corrected for water vapor using the water channel of the LI-COR detector. The instrument was operated in the absolute mode and gathered CO_2 concentrations directly from the instrument. The LI-COR instrument analyzes the concentration of CO_2 every 6 s, then averaged these values over a 5-min interval, and recorded them. Atmospheric air was pumped at the bow of the ship and measured every hour. The system was calibrated by measuring two different standard gases with mixing ratios of 348.55 and 520.83 ppm CO_2 in the air. These calibrated standards were provided by the National Oceanographic and Atmospheric Administration and they are traceable to the World Meteorology Organisation scale. Our system demonstrated a precision of less than $1 \mu\text{atm}$ and was accurate, relative to standard gases, to $2 \mu\text{atm}$. Fugacity of CO_2 in the seawater was calculated from the measured $x\text{CO}_2$ (mol fraction of CO_2 gas corrected to dry air and to the pressure of 1 atm).

2.3. Dissolved Oxygen and Nutrient Measurements

[12] Dissolved oxygen was measured using an automated potentiometric modification of the original Winkler method following World Ocean Circulation Experiment (WOCE) standards [*WOCE*, 1994]. The standard error for five replications was lower than $2 \mu\text{mol/kg}$. The apparent oxygen utilization (AOU), defined as the deficit of oxygen concentration in proportion to atmospheric saturation [*United Nations Educational, Scientific, and Cultural Organization*, 1986], was used to describe the oxygen distributions.

[13] Samples for nutrient analysis were frozen at -20°C and then analyzed in the laboratory following WOCE standards [*WOCE*, 1994]. Nutrients were determined by colorimetric methods, using a Technicon AutoAnalyzer AAII. For silicate, a modified *Hansen and Grasshoff* [1983] method was used, in which β -silicomolybdenic acid was reduced with ascorbic acid. Nitrate was determined after reduction to nitrite in a Cd-Cu column. The standard deviation for duplicates was $0.07 \mu\text{mol/l}$ for silicate, $0.06 \mu\text{mol/l}$ for nitrate, and $0.01 \mu\text{mol/l}$ for phosphate representing a reproducibility of 0.3, 0.5, and 0.8%, respectively. The method of dissolved organic carbon, particulate organic carbon and particulate organic nitrogen analysis is described by *Dafner et al.* [1999]; the method of phytopigments determination is presented by *Gómez et al.* [2000].

3. Results and Discussion

3.1. Hydrology

[14] Meteorological conditions during sampling were marked by storm events accompanied by an east wind with a speed of about $15 \pm 3 \text{ m s}^{-1}$ and an average pressure of 1024 mbar. The dynamic environments were affected by these events because of mixing in the surface layer. The dominant feature of temperature and salinity distribution across this section is a well-mixed layer which extends down to the bottom, at the shelf stations 1 and 2, and to approximately 140 m depth at the offshore stations 3 to 5 (Figure 2).

[15] In the mixed layer, two different water masses were found. The first water mass is the Gulf of Cadiz Water (GCW) or Iberian Continental Shelf Water, which is char-

acterized by a temperature of 16.14°C and salinity of 36.06 – 36.10. The lower value of salinity in the GCW (station 1) suggests there is an influence of river discharge in the Gulf of Cadiz area. The influence of river discharge during the formation of the GCW has been described in more detail by *Van Geen et al.* [1988, 1991]. The second surface water mass is the North Atlantic Surface Water (NASW), with a temperature of 17.12°C and salinity of 36.46. The thickness of the NASW in February 1998 was determined by the strong wind, which produced a well-mixed layer down to 140 m. Interaction between the GCW and NASW produces a front which is located close to the break of the shelf. Figure 2 shows that the distribution of the GCW is restricted by the shelf waters located around station 1 and this water mass does not affect the distribution of salinity and temperature at the offshore stations. The North Atlantic Central Water (NACW) was found at stations 4 and 5 between 250 and 400 m depth, and is defined by a minimum of both salinity (<36.00) and temperature (<13.80°C). The coldest and least saline NACW overlays the Mediterranean waters and underlies NASW, producing a large thermohaline gradient.

[16] Mediterranean water (MW) is characterized by high salinity and temperature (37.07 and 15.30°C), increasing in density close to the bottom layer (to 27.34 at station 3 and to 27.56 kg m⁻³ at station 4). In this area, *Ambar and Howe* [1979a, 1979b] observed that “the T-S distribution definitely reveals the initial stage in the subdivision of the MW into two cores. The lower main core (ML) can be identified characteristically by the maximum salinity of 37.42 at a depth of 756 m (T = 13.16°C, σ_o = 28.28), whereas the upper core (Mu) appears between 500 and 650 m, with a temperature as high as 13.72°C at 650 m (S = 37.07, σ_o = 27.88).” The density values we found in February 1998 are significantly lower than those presented by *Ambar and Howe* for the upper core of the Mediterranean outflow.

[17] To explain this difference in density, we refer to other work of *Ambar* [1983]. She analyzed several sets of hydrological data taken in the Gulf of Cadiz and off the western coast of Portugal, and identified the continuity of a shallow vein of MW, distinct from two, already well-established, main cores. She has characterized the shallow core of MW at density levels between 27.25 and 27.45 kg m⁻³ with an equilibrium depth between 400 and 700 m, and with a thickness of 50 to 100 m [*Ambar*, 1983]. A comparison of density values suggests that in February 1998 we observed the third, the shallow core, of Mediterranean outflow. *Ambar and Howe* [1979a, 1979b] have studied the Mediterranean outflow only from the depth of >600 m and they could not find the shallow core in the area located above the slope. The bottom contour in Figure 2 suggests that this section is located above a valley, and temperature and salinity distributions show that the Mediterranean outflow spreads along the bottom and the continental slope according to the Coriolis deflection.

3.2. Carbonate System in Relation to Different Water Masses

[18] The four water masses previously described and defined by their thermohaline properties (Figure 2), are also characterized by a different carbonate system (Figure 3) and nutrient values (Table 1 and Figure 4). The GCW, with low salinity values at station 1 due to the river influence is traced

by high A_T (2397 $\mu\text{mol kg}^{-1}$) and C_T (2105 $\mu\text{mol kg}^{-1}$) and relatively low $\text{pH}_{T-25^\circ\text{C}}$ value (7.970). The influence of river discharge on A_T and C_T distributions has already been discussed for the Mediterranean Sea by *Pérez et al.* [1986] who found alkalinity values as high as 2703 $\mu\text{mol kg}^{-1}$ (S = 33.14) close to the Ebro river. There are no alkalinity values in coastal waters for this area. However, if we apply a mass balance for salinity between river outflow and station 1 (depth of 50 m) assuming conservative behavior for alkalinity, a value of $A_T^{S=0} = 3430 \mu\text{mol kg}^{-1}$ was determined. Considering conservative behavior for alkalinity, after removing fresh water effect, surface NA_T was $2290 \pm 1 \mu\text{mol kg}^{-1}$ in the full area. The GCW is also distinguished by high silicate concentration (Figure 4) and negative AOU values within the water column (Figure 3d). Negative values of AOU over the shelf and in surface waters show these waters were over-saturated with oxygen and high values of Chl *a* in Table 1 show that this reading is affected by the photosynthetic activity of phytoplankton. The shallow core of Mediterranean outflow, which restricts the penetration of NACW to the slope, produces large thermohaline as well as carbonate system variable gradients (Figure 3).

[19] The Mediterranean outflow is characterized by high values of A_T (Figure 3a) and NA_T at the bottom of the valley ($NA_T \sim 2315 \mu\text{mol kg}^{-1}$, station 4). The MW spreads along the slope up to station 3, where the values of A_T (Figure 3a) and NA_T in the near-bottom layer are still high ($NA_T \sim 2305 \mu\text{mol kg}^{-1}$). NASW is distinguished by low NA_T values (<2295 $\mu\text{mol kg}^{-1}$), low NC_T ($\sim 2005 \mu\text{mol kg}^{-1}$), and high pH_{T-25} values (7.985). NACW is specifically characterized by high silicate concentration around 300–400 m with values as high as 5.2 $\mu\text{mol kg}^{-1}$, high AOU values (53 $\mu\text{mol kg}^{-1}$, Figure 3d), and low $\text{pH}_{T-25^\circ\text{C}}$ values (7.833).

[20] Figure 4 depicts the scatterplots between different properties. The relationships between potential temperature and salinity as well as the relation between NA_T (the river effect has not been removed) and silicate (Figure 4b) clearly identify the different water masses. The highest NA_T and relatively high silicate values are characteristic of the GCW (station 1). Intermediate values of NA_T correspond to the MW and water under its influence, while the lowest NA_T and silicate values are typically found at the NASW. The presence of NACW is well defined by the highest silicate concentrations at station 5.

[21] No documented values for the carbonate system variables measured in the Gulf of Cadiz have been found. Values of NA_T for NACW with salinity of approximately 35.72 of 2296 $\mu\text{mol kg}^{-1}$ at 37°35'N 21°33'W (M. González-Dávila, unpublished data, 1999) and 2295 $\mu\text{mol kg}^{-1}$ at 37°52.6'N 17°27.8'W [*Transient Tracers in the Ocean*, 1981] coincide with our findings at station 5. Similar values of NA_T (2313 to 2317 $\mu\text{mol kg}^{-1}$) to those reported here for the MW were found in the Mediterranean outflow within the same range of salinity in the western entrance of the Strait of Gibraltar [*Santana-Casiano et al.*, 2002]. In the Alboran Sea, where salinity values correspond to the shallow core (37.07), *Copin-Montégut* [1993] has also observed similar values of NA_T ranging from 2304 to 2315 $\mu\text{mol kg}^{-1}$.

3.3. Relationships Between CO₂ and Nutrients

[22] A number of researchers have examined the A_T and C_T of oceanic waters using semi-empirical equations as

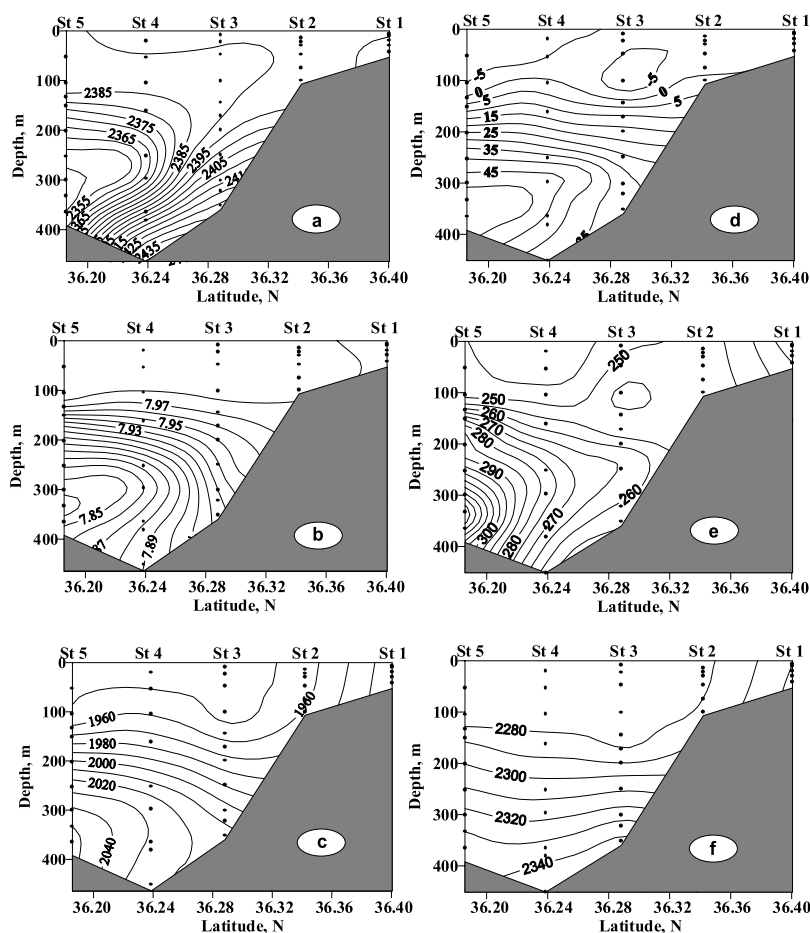


Figure 3. Cross-slope distribution of data presented in Table 1. (a) A_T ($\mu\text{mol kg}^{-1}$), (b) $\text{pH}_T-25^\circ\text{C}$ (mol (kg-SW)^{-1}), (c) normalized preindustrial total inorganic carbon NC_T^0 ($\mu\text{mol kg}^{-1}$), (d) apparent oxygen utilization, AOU ($\mu\text{mol kg}^{-1}$), (e) the conservative parameter NO ($\mu\text{mol kg}^{-1}$), and (f) the conservative parameter referring to preindustrial values NCO^0 ($\mu\text{mol kg}^{-1}$) along the section at the traverse of Cadiz (10–11 February 1998, Gulf of Cadiz).

functions of salinity, temperature, nutrients, and oxygen [Brewer *et al.*, 1995; Wallace, 1995; Millero *et al.*, 1998]. These equations can be used to make reasonable extrapolations of C_T and A_T from the most commonly measured hydrographic and nutrient properties and thus show the internal consistency of the measurements. In this sense we have studied the relationship between carbon dioxide and nutrient measurements taken in this study.

[23] C_T , dissolved oxygen and nutrients are involved in primary production and regeneration of organic material. Moreover, their levels of concentration depend on when the water mass was last ventilated. The Redfield ratios of remineralization determined for the Northeast Atlantic Ocean (3°N – 41°N) by Körtzinger *et al.* [2001] of $-\text{O}_2:\text{C}_{\text{org}}$ of 1.34, $\text{C}_{\text{org}}:\text{N}$ of 7.2 were considered in this study after correcting concentrations of dissolved inorganic carbon to preanthropogenic conditions. In order to remove the anthropogenic increase of CO_2 on the dissolved inorganic carbon concentrations, the improvements on the back-calculation technique proposed by Pérez *et al.* [2002] were applied. The preanthropogenic C_T , thus computed is presented in Table 1 and plotted in Figure 3c normalized to a constant salinity of 35. Figure 4 shows the

covariation of concentrations of NC_T^0 versus nitrate plus nitrite and phosphate. Despite the participation of both CO_2 and nutrients in biological processes, and the scarce quantity of C_T^0 observations ($N = 34$), these correlations exhibit a systematic relationship. The regression analysis after removing station 1, which is affected by river inputs, yields normalized preanthropogenic C_T concentrations at zero nutrients (Figure 4) of $1951 (\pm 3)$ and $1949 (\pm 6) \mu\text{mol kg}^{-1}$ which represents, primarily, the pre-anthropogenic effect of CO_2 solubility plus a lower effect of the CaCO_3 dissolution. Our anthropogenic calculation gives anthropogenic carbon concentrations between 55 and $35 \mu\text{mol kg}^{-1}$ from the near surface to 500 m, respectively. For the Gulf of Cadiz, we calculated that the quantity of inorganic carbon in the water column contributed by the dissolution of carbonate particles (following Sabine *et al.* [1995]) was $6 \mu\text{mol CO}_2 \text{ kg}^{-1}$ increasing at the bottom of station 4 to $10 \mu\text{mol CO}_2 \text{ kg}^{-1}$. In the North Atlantic main thermocline water, Takahashi *et al.* [1985] found that the influence from the effects of CO_2 solubility plus the CaCO_3 dissolution could be as high as $8 \mu\text{mol CO}_2 \text{ kg}^{-1}$.

[24] The $\text{pH}_T-25^\circ\text{C}$ correlates with N_T and P giving a surface estimate of $\text{pH}_T-25^\circ\text{C}$ as $8.000 (\pm 0.004)$ (Figure 4).

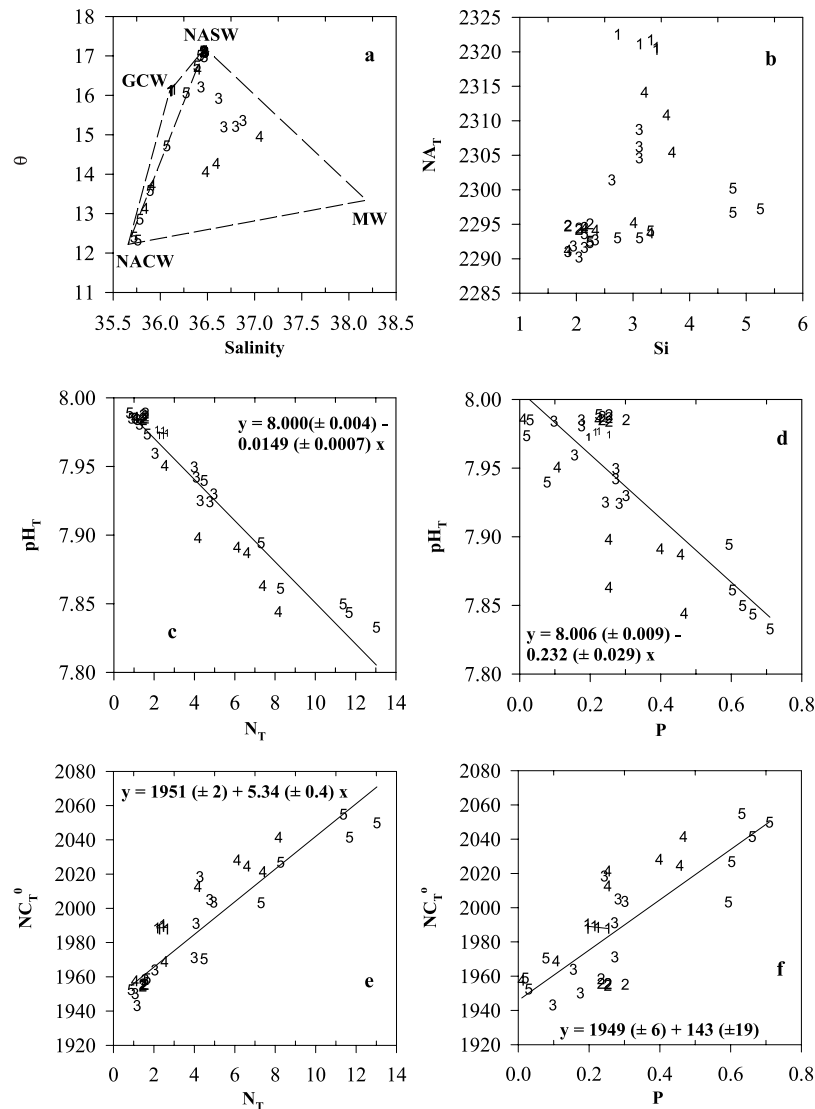


Figure 4. Relationship between (a) potential temperature (θ) and salinity, (b) NA_T ($\mu\text{mol kg}^{-1}$) and silicate ($\mu\text{mol kg}^{-1}$), (c) pH_T -25°C and N_T ($\mu\text{mol kg}^{-1}$), (d) pH_T -25°C and P_T ($\mu\text{mol kg}^{-1}$), (e) normalized preindustrial total inorganic carbon, NC_T^0 ($\mu\text{mol kg}^{-1}$) and N_T ($\mu\text{mol kg}^{-1}$), and (f) NC_T^0 ($\mu\text{mol kg}^{-1}$) and P ($\mu\text{mol kg}^{-1}$).

Oxidation of the sinking organic particles consumes oxygen and produces protons, resulting in the pH_t decrease [Sabine *et al.*, 1995].

3.4. Influence of Gulf of Cadiz Water and Mixing on A_T and C_T Chemistry

[25] As we have already seen, thermohaline, nutrients, oxygen and carbonate system variables across the shelf (stations 1 and 2) were affected by the Gulf of Cadiz water. In this section, we will analyze other biogeochemical parameters, such as particulate organic carbon and nitrogen (POC and PON) and phytopigments (Chl *a* and phaeopigments) in relation to A_T and C_T properties. The dominant feature of particulate organic matter (POM) distribution is the very high concentrations across the shelf (Table 1). Concentrations of POC and PON at station 1 vary slightly over the water column from 19 $\mu\text{M C}$ and 1.4 $\mu\text{M N}$ at the surface (10 m) to 22 $\mu\text{M C}$ and 1.6 $\mu\text{M N}$ in the bottom

layer (42 m). The POC/PON ratios in Table 1 illustrate that the observed values (5.7–8.0) were only close to the classic Redfield ratio of 6.6 indicating organic matter (OM) from plankton at stations 2 and 3. At the other stations, C/N ratios were up to and over 2 or 3 times the Redfield values, suggesting the POM was already partly degraded.

[26] It is a well-documented fact that fresh algal material is characterized by Chl *a*, whereas degraded phytoplankton is characterized by phaeopigments (chlorophyllide-phaeophytin-phaeophorbide, hereinafter Phaeo). During the period of sampling, oceanographic conditions in this area were influenced by storm events. Figure 5 demonstrates homogeneous distribution of Chl *a* in the well-mixed layer in the top 100 m (0.30–0.50 $\mu\text{g L}^{-1}$) while concentrations of Phaeo decrease from station 1 to station 5 (1.12 to 0.07 $\mu\text{g L}^{-1}$). Negative values of AOU, high contents of POC, PON, and Chl *a* over the shelf (station 1) suggest that there is photosynthetic activity in this water. Nutrient discharge from rivers and

Table 1. Five Stations Sampled at the Traverse of Cádiz With Nominal Depths of Sampling (H, m) and Values of Temperature ($^{\circ}\text{C}$), Salinity, A_T ($\mu\text{mol kg}^{-1}$), pH_T (mol (kg-SW) $^{-1}$), C_T and Pre-Anthropogenic C_T° ($\mu\text{mol kg}^{-1}$), $f\text{CO}_2$ (μatm), Apparent Oxygen Utilization (AOU, $\mu\text{mol kg}^{-1}$), N_T ($\text{NO}_2^- + \text{NO}_3^-$), PO_4^{3-} , Si (All Nutrients in $\mu\text{mol kg}^{-1}$), DOC, POC, PON (All in μM), POC/PON Ratio (PC/PN), Chl a and Phaeo (Both in $\mu\text{g L}^{-1}$)

Station	H	T	S	A_T	pH_T -25	C_T	C_T°	$f\text{CO}_2$	AOU	N_T	PO_4^{3-}	Si	DOC ^a	POC ^a	PON ^a	PC/PN	Chl a^a	Phaeo ^a
1	7	16.11	36.10	2397	7.972	2105		338	-5.26	2.43	0.19	3.4	61	19	1.4	13.6	0.506	0.81
	10	16.11	36.10	2397	7.972	2105	2051	338	-3.75	2.24	0.19	3.1	89	21	1.6	13.1	0.525	0.85
	20	16.11	36.10	2396	7.974	2103	2050	336	-3.04	2.63	0.25	3.4	64	21	1.6	13.1	0.475	1.07
	29	16.13	36.11	2398	7.976	2104	2053	334	-2.23	2.43	0.21	3.3	65	22	1.6	13.8	0.448	1.12
	42	16.15	36.14	2398	7.976	2106	2053	334	-3.65	2.14	0.22	2.7	64	-	-	-	0.545	0.89
2	14	17.11	36.46	2390	7.986	2091	2037	337	-1.24	1.56	0.25	2.1	63	-	-	-	0.485	0.32
	22	17.11	36.46	2391	7.987	2090	2037	336	-1.24	1.46	0.23	1.8	64	3	0.4	7.5	0.466	0.31
	30	17.11	36.46	2390	7.988	2089	2037	335	-0.94	1.56	0.25	2.0	63	5	0.9	5.6	0.485	0.32
	48	17.12	36.46	2390	7.984	2092	2036	340	-2.15	1.46	0.25	2.0	-	-	-	-	0.429	0.42
	75	17.11	36.46	2391	7.985	2092	2037	338	-2.05	1.46	0.30	1.8	64	4	0.8	5.0	0.485	0.34
	100	17.13	36.46	2392	7.985	2092	2040	339	2.10	1.56	0.23	2.2	63	4	0.8	5.0	0.504	0.35
3	9	17.1	36.47	2387	7.981	2091		342	-9.86	1.27	0.17	2.0	48	-	-	-	0.446	0.11
	23	17.1	36.47	2392	7.981	2095		343					48	-	-	-	0.445	0.09
	48	17.11	36.47	2388	7.985	2089	2032	338	-4.62	1.07	0.17	1.8	54	-	-	-	0.418	0.07
	101	17.11	36.47	2388	7.984	2090	2025	339	-4.94	1.17	0.10	1.9	55	4	0.5	8.0	0.348	0.11
	144	17.12	36.47	2389	7.973	2098		350					-	-	-	-	0.373	0.25
	172	17	36.46	2388	7.959	2104	2046	361	11.6	2.04	0.17	2.1	53	4	0.6	6.7	0.165	0.15
	199	16.24	36.43	2386	7.950	2109	2052	359	9.73	3.99	0.27	2.3	58	5	0.8	6.3	0.052	0.08
	250	15.96	36.61	2408	7.942	2132	2083	365	26.2	4.08	0.27	2.6	65	-	-	-	0.043	0.07
	301	15.24	36.67	2415	7.930	2143	2099	363	31.0	4.96	0.30	3.1	62	-	-	-	0.049	0.06
	322	15.26	36.79	2425	7.924	2155	2108	370	33.1	4.76	0.28	3.1	55	5	0.7	7.1	0.052	0.07
	352	15.41	36.87	2432	7.925	2163	2126	376	31.7	4.28	0.24	3.1	58	-	-	-	0.051	0.09
4	20	17.12	36.47	2391	7.982	2094		342					61	-	-	-	0.354	0.22
	54	17.13	36.47	2391	7.985	2092		339	-5.74	1.07	0.22	2.1	60	-	-	-	0.373	0.25
	105	17.12	36.47	2388	7.986	2089	2040	337	5.15	1.07	0.01	1.8	57	7	0.4	17.5	0.317	0.21
	162	16.69	36.39	2386	7.950	2108	2047	365	10.5	2.53	0.11	2.3	54	-	-	-	0.041	0.07
	252	13.75	35.91	2354	7.863	2129	2074	405	37.3	7.39	0.25	3.3	49	-	-	-	0	0.02
	297	13.17	35.83	2350	7.844	2136	2090	416	54.3	8.17	0.47	3.0	49	8	0.4	20.0	6E-04	0.02
	365	14.11	36.48	2403	7.884	2161	2110	394	41.4	6.61	0.46	3.7	49	6	0.4	15.0	0.026	0.04
	382	14.32	36.59	2416	7.888	2170	2121	395	44.7	6.12	0.40	3.6	57	-	-	-	0.023	0.04
	451	15.02	37.05	2450	7.904	2198	2131	409	35.1	4.18	0.25	3.2	52	7	0.4	17.5	0	0.08
5	52	17.13	36.45	2387	7.989	2087		335	-3.85	0.78	0.22	2.2	62	-	-	-	0.485	0.07
	105	17.03	36.42	2386	7.985	2088	2032	337	-4.88	0.88	0.03	2.2	64	5	0.5	10.0	0.373	0.05
	134	16.76	36.38	2385	7.973	2094	2036	343	-1.46	1.65	0.02	2.1	64	-	-	-	0.094	0.02
	151	16.09	36.27	2376	7.940	2107	2042	366	4.56	4.48	0.08	2.7	61	-	-	-	0.034	0.01
	202	14.75	36.06	2363	7.894	2121	2064	390	28.6	7.30	0.59	3.1	65	3	0.3	10.0	0.006	0.01
	253	13.62	35.89	2352	7.861	2129	2078	405	42.4	8.27	0.60	3.3	54	-	-	-	0.005	4e-3
	300	12.89	35.78	2348	7.844	2135	2087	411	48.4	11.7	0.66	4.8	55	3	0.2	15.0	0.008	5e-3
	333	12.45	35.72	2344	7.833	2137	2092	414	52.7	13.0	0.71	5.2	53	-	-	-	0.002	3e-3
	365	12.37	35.76	2350	7.850	2134	2100	394	55.9	11.4	0.63	4.8	53	3	0.2	15.0	0	0.01

^aThese data were withdrawn from *Dafner et al.* [1999].

nutrients from sediment pore waters could have supported the biological production. The shelf waters at station 1 were characterized by higher Phaeo concentrations (up to $0.95 \mu\text{g L}^{-1}$, on average) than Chl a ($0.5 \mu\text{g L}^{-1}$, on average) while at station 2, by contrast, values of Chl a exceeded concentrations of Phaeo (0.48 and $0.34 \mu\text{g L}^{-1}$, on average). Those values of POC/PON ratios in Table 1 that exceed 10 support the hypothesis that the sources of these phytopigments probably derive from river output across the shelf rather than from phytoplankton growing on the shelf [*Parsons et al.*, 1977]. This material may constitute an easily resuspended layer at the water-sediment interface under strong wind conditions.

[27] A curvature of isolines in Figure 5 suggests some slope of isoline of phytopigments between stations 3 and 4. Additionally, an examination of the AOU, Chl a and Phaeo values in Table 1 shows slightly increased concentrations of Phaeo in the near-bottom layer at stations 3 and 4. Our working hypothesis is, therefore, that the increase of near-bottom concentrations of phytopigments that is also accompanied by relatively low AOU values could be due to an

along-slope descent of the shelf waters. This hypothesis has a significant implication for the MW. Shelf waters may be a very important source of OM to the MW influencing the biogeochemistry of the MW and consequently, the eastern North Atlantic during winter. A similar conclusion has been presented by *Ambar et al.* [1976]. Describing the hydrological structure in the area close to the Saõ Vicente Cap, they found the presence of water of shallow origin at depths of between 450 and 580 m. They hypothesized that these anomalously high temperatures and salinity values were due to winter cooling and a consequent sinking of this water from the shelf. To check our hypothesis, we need to investigate further with smaller spatial resolution sampling to avoid gaps in the data on the slope.

3.5. Mixing Analysis of Nutrients and Inorganic Carbon

[28] As we pointed out above, four sources of water influence the physical and chemical composition of the Gulf of Cadiz: (1) Atlantic surface waters, (2) North Atlantic Central waters, (3) Gulf of Cadiz water, and

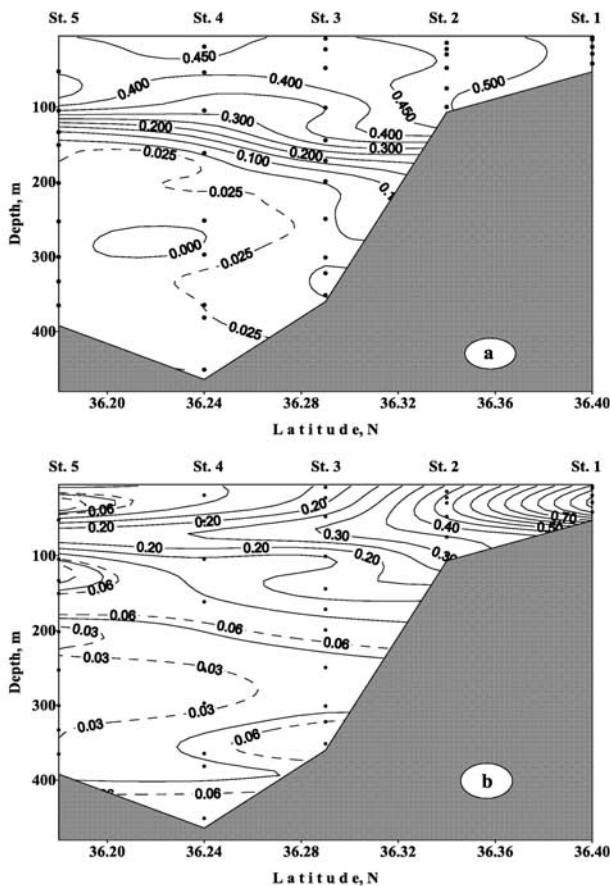


Figure 5. Cross-slope distribution of (a) Chlorophyll *a* and (b) phaeopigments ($\mu\text{g L}^{-1}$) at the traverse of Cadiz.

(4) Mediterranean waters. The thermohaline properties of these water masses have been extensively described in previous studies [Madelaine, 1967; Zenk, 1975; Ambar *et al.*, 1976; Ochoa and Bray, 1991; Price *et al.*, 1993]. In this study, we combined thermohaline and chemical properties to study the chemical variability of this area. Several mixing models can be used to quantify the variability of both nutrient and inorganic carbon system features, using the water masses variability followed by thermohaline distribution (Figure 4a).

[29] Tomczak [1981] developed seawater analysis using mixing triangles without assumption of isopycnal mixing. This kind of analysis can only resolve mixing from three end members, as only salinity and temperature will be used as conservative variables [Pérez *et al.*, 1998]. Each water end member is defined by a single and fixed temperature and salinity while a water mass is conventionally characterized by the mixing of two end members, thus showing a rather fixed T-S relationship. Alternatively, if the profile of water masses is perfectly well defined by the thermohaline variability, it is possible to define a mixing model that is based on a set of vertically ordered mixing triangles.

[30] Following the water masses description given above, we define a set of end members in order to describe thermohaline variability due to mixing. It is not necessary to assume either isopycnal or diapycnal mixing. Figure 4a shows the θ -S diagram, after removing samples from the

first 100 m depth. A high correlation θ to S between NASW and NACW is observed,

$$\theta = (6.32 \pm 0.07)S - (213.4 \pm 2.7) \quad r^2 = 0.996, N = 17.$$

We chose the pairs of salinity and potential temperature values of 36.474, 17.20 and 35.66, 12.22 for the end members of NASW and NACW, similar to those used by Van Geen *et al.* [1988] for this area. The GCW was defined by the salinity and potential temperature obtained in station 1 (36.1 and 16.11). For the Mediterranean water, the salinity and potential temperature (38.18 and 13.34) was selected adopting mean values observed in the Strait of Gibraltar [Santana-Casiano *et al.*, 2002]. Given that the distribution of thermohaline and chemical parameters are strongly influenced by the spreading of MW in the area, we used the triangular mixing approach for NASW-NACW-MW to estimate the contribution of the MW [Pérez *et al.*, 1998]. Only eight samples were inside this triangle, which were considered for the further mixing analysis (Figure 4a).

[31] In order to support the proposed mixing model, we have applied the model to the conservative tracer NO ($\text{NO} = \text{O}_2 + \text{N}_T \times \text{R}_N$) with a R_N of 9.33 [Fraga *et al.*, 1998; Körtzinger *et al.*, 2001] to eliminate the effect of remineralization of organic matter on the nitrate and oxygen variability (Figure 3e). The mixing model explains 98.1% of NO variability (Table 2). The standard deviation of NO residuals ($7 \mu\text{mol kg}^{-1}$) is about twice the expected error due to reproducibility of nitrate and oxygen ($0.06 \times 10 + 2 = 2.6 \mu\text{mol kg}^{-1}$) and lower than the expected from the combination of the residuals of nitrate and oxygen ($9 \mu\text{mol kg}^{-1}$). If we use the chemical tracer $\text{NCO}^\circ = \text{NO} + \text{C}_T^\circ \times \text{R}_{\text{CS}} - \text{N}_T \times \text{R}_N \times \text{R}_{\text{CS}}/\text{R}_C$ [Rios *et al.*, 1998] (Figure 3f), calculated considering the anthropogenic contribution to C_T and where R_{CS} is the relationship between oxygen consumed and CO_2 assimilated corresponding to storage substances (generally carbohydrates with a $\text{R}_{\text{CS}} = 1$ [Rios *et al.*, 1998]), the mixing model explains 98.7% of NCO° variability (Table 2). The standard deviation of NCO° residuals ($5.1 \mu\text{mol kg}^{-1}$) is twice as low as expected from the combination of the residuals of NO, nitrate and CO_2 (Table 2). The distribution of both NO and NCO° residuals (data not shown) does not show a clear relation with the distribution of NO and NCO° or any other biogeochemical variable. The high variability of NCO° predicted by the mixing model supports the quality of the model.

[32] The contribution of Mediterranean water to the eight samples affected varied from 15% to 40%. The highest value (40%) was observed at the bottom of station 4, decreasing to 30% at the bottom of station 3. The chemical end-member characteristics, after applying the mixing model, are shown in Table 2. The variance explained by the application of the model for the distribution of carbonate system variables and nutrients was more than 94.9%, while the variance explained for alkalinity (after removing nitrate alkalinity) was as high as 99.5%. The difference in the proportion of not-explained variability was related to both the magnitude of the total natural variance of each chemical tracer and non-conservative behavior. The model clearly defines the alkalinity end members and its natural variability. Errors of both alkalinity end members and residuals are close to the analytical errors.

Table 2. Definition of the Three Water Types and Their Characteristics as a Result of the Mixing Model Over the Eight Water Samples

	S	T	A _T	C _T ^o	AOU	pH _T -25	N _T	PO ₄ ³⁻	Si	NO	NCO ^o
NASW ^a	36.474	17.20	2384 ± 1	2038 ± 4	-2	7.978 ± 0.006	2.7 ± 0.2	0.19 ± 0.11	1.7 ± 0.5	245 ± 2	2265 ± 4
NACW	35.660	12.22	2342 ± 1	2096 ± 3	50	7.839 ± 0.004	10.6 ± 0.3	0.22 ± 0.12	4.7 ± 0.7	362 ± 2	2385 ± 3
MW	38.185	13.34	2556 ± 1	2273 ± 3	22	7.867 ± 0.004	4.9 ± 0.3	0.8 ± 0.13	5.1 ± 0.7	268 ± 3	2507 ± 4
r ²			0.995	0.949	0.94	0.963	0.965	0.981	0.967	0.981	0.987
Std			1.3	5.1	3.7	0.005	0.2	0.11	0.01	7.0	5.1

^aNASW after removing the first 100-m-depth samples.

[33] The end members summarize the chemical variability of the water masses. The high nutrient levels and low pH_T in NACW contrasts with that of MW, with higher pH_T-25°C and intermediate nitrate values. In contrary to NO and NCO^o, the variability in the nutrient residuals (real minus modeled values) can be ascribed to either remineralization of organic matter (ROM) or dissolution of hard parts of biogenic matter. The AOU distributions clearly showed the patterns of the ROM accumulated in the water masses since formation.

[34] The correlation between phosphate and nitrate residuals was 0.53 with a N:P ratio of 14.6 ± 0.7. Ratios C_T^o to nitrate and C_T^o to phosphate also show a significant correlation (0.52 and 0.61) with a C:N ratio corrected to preanthropogenic conditions of 6.4 ± 0.5 and a C:P ratio of 99 ± 5. The small amount of data, small resolution of sampling and the good fit of the model yields low variances of the residuals, and therefore a high correlation between them should not be expected. However, our ratios are close to those reported by *Körtzinger et al.* [2001] of N:P, 17.5 ± 2, C:P, 122 ± 12 and C:N, 7.2 ± 0.8. Differences in the reported ratios may be due to regional patterns associated with the input of nitrate and phosphorus from sediment remobilization. Given the limitations of the present data set, we cannot solve this difference here and further work was necessary.

3.6. The fCO₂ in the Gulf of Cadiz During the Winter Events

[35] Figure 6 shows fCO₂ in surface water and in the atmosphere and the sea surface temperature recorded during the Gulf of Cadiz section. The mean fCO₂ concentrations in the seawater were 330.6 ± 5.6 μatm, while the CO₂ content of the air was very stable (365.4 ± 0.7 μatm). With these values, an average ΔfCO₂ of -35 μatm was calculated, showing that this area was acting as a sink of CO₂ at this time of the year. The observed fCO₂ difference between the surface ocean and the atmosphere represents the thermodynamic driving potential for CO₂ transfer across the sea surface and includes, implicitly, the combined effects of all the processes that influence CO₂ distribution in the ocean and atmosphere [*Tans et al.*, 1990].

[36] The transfer velocity relationship of *Wanninkhof* [1992] was used to provide CO₂ flux calculations,

$$k = 0.31 w_{10}^2 (Sc/660)^{-0.5},$$

where Sc was the Schmidt number for CO₂ and w₁₀ was the wind speed at 10 m height (in m s⁻¹). The primary environmental variables that determine the flux are the wind speed, total atmospheric pressure, and the air-sea CO₂ difference. Wind speed data were gathered at 1-min

intervals from the meteorological shipboard facilities, while atmospheric pressure values were obtained from our system. The CO₂ solubility and Schmidt number were taken from *Weiss* [1974] and *Wanninkhof* [1992], respectively. Meteorological parameters were taken from the shipboard data-acquisition system, and averaged hourly. The averaged wind speed was 15 ± 3 m s⁻¹.

[37] The computed CO₂ flux is shown in Figure 6. A net carbon dioxide flux of -19.5 ± 3.5 mmol m⁻² d⁻¹ was obtained for the area. Owing to the storm conditions at this time of the year, with stable but high wind speed, CO₂ flux was controlled by the fugacity difference (Figure 6). Station 1, located on the shelf, presents the inflow of cold Gulf of Cadiz water with a temperature 1.0°C lower than sea surface temperature on offshore stations, and Chl *a* concentration of 0.51 μg L⁻¹ (Table 1) resulting in a mean fugacity value of 328 ± 2 μatm. Toward the west (stations 2 to 5), the temperature increases 1.0°C (up to 17.10°C), and as a result the fCO₂ decreases from 338 μatm at station 2 to 325 μatm at station 5, which is farthest offshore. If the fCO₂ values are normalized to a constant temperature of 17.1°C, station 1 reaches 342 μatm following the observed trend.

3.7. Estimates of C_T Transport Within the Mediterranean Outflow

[38] The study of carbon transport by the Mediterranean outflow in this area was of special interest. On leaving the Gulf of Cadiz, the Mediterranean outflow enters into the interior of the open ocean at the intermediate depth as tongue and lenses of salty waters which are widespread

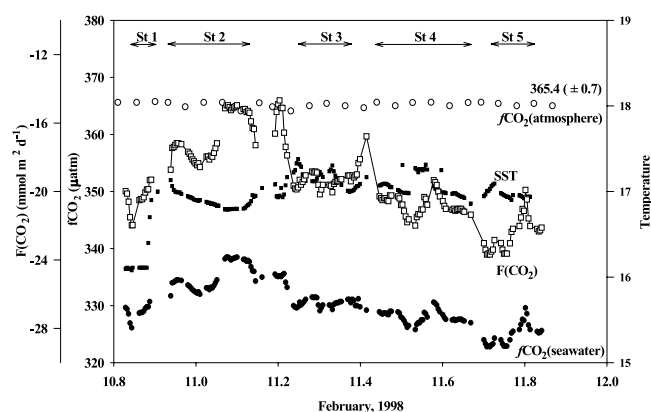


Figure 6. Mesoscale distribution of sea surface fCO₂ (solid circles), atmospheric fCO₂ (open circles), and sea surface temperature (SST, solid small squares) along the section at the traverse of Cadiz (10–12 February 1998). Computed net CO₂ flux (F, large open squares) across the air-sea interface was also included.

along the North Atlantic [Arhan *et al.*, 1994; Ambar and Howe, 1979b]. Little is yet known about the influence of the Mediterranean water on the biogeochemistry of the North Atlantic and on the carbon cycle in particular.

[39] The shallow core is one of the least studied cores of the Mediterranean outflow. It has been described only in the terms of thermohaline parameters, not providing any information on mass transport [Ambar, 1983]. In this study, we used the velocity range 10 to 20 cm s⁻¹, which had been presented by a number of authors for the upper core of the Mediterranean outflow in this area [Ambar and Howe, 1979b; Ochoa and Bray, 1991], and a C_T value of 2198 μmol kg⁻¹. Our estimate for the shallow core of MW transport (considering the geometry of the section) ranges from 5.2 × 10³ to 10.4 × 10³ m³ s⁻¹, which corresponds to 1.2 × 10⁴ to 1.4 × 10⁴ mol C s⁻¹. It has been shown that the average C_T outflow across the Strait of Gibraltar was about 11.9 × 10⁴ mol C s⁻¹ [Dafner *et al.*, 2001]; that is, carbon transport by the shallow core was 1 order of magnitude lower than for the Mediterranean outflow in the Strait of Gibraltar. For this section, dissolved organic carbon transport by the shallow core has been estimated to be 2 orders of magnitude lower than that found in the Strait of Gibraltar [Dafner *et al.*, 1999].

4. Conclusions

[40] The Gulf of Cadiz is a unique area of the eastern North Atlantic for the study of the carbon cycle with small spatial and temporal resolutions. Its wide and shallow shelf, river discharge, the formation of the Atlantic inflow flowing into the Mediterranean Sea, and the transition of the Mediterranean outflow on its way into the open ocean all combine to produce an area of unparalleled interest. Our winter meso-scale measurements of carbonate system properties at the traverse of Cadiz were carried out during storm events which were accompanied by strong winds and a well-mixed layer. The inorganic carbon chemistry was affected by the interaction of different water masses and the mineralization of organic material. We assume that the sources of organic matter on the shelf are accumulated either from the river input or spring-summer production by phytoplankton. We hypothesize that the source of OM in deep waters, including the shallow core, was descending off the shelf waters during winter mixing. Application of the simple mixing model for the NASW-NACW-MW water masses explains more than 96% of the variability of chemical properties.

[41] Large variability of instantaneous *f*CO₂ in the surface seawater was observed with fine temporal and spatial scales. The difference of *f*CO₂ between seawater and atmosphere shows that the surface seawater in the Gulf of Cadiz was a sink for atmospheric CO₂ during winter events. The calculated net CO₂ flux across the air-sea interface is, on average -19.5 ± 3.5 mmol m² d⁻¹.

[42] The shallow core presents a small part of Mediterranean water outflowing from the Mediterranean Sea. The Mediterranean outflow was affected by the entrainment of NACW resulting in decreases of the amount of inorganic carbon in the outflow. Owing both to entrainment and to the ageostrophic character of the outflow near the strait, the transport of inorganic carbon in the Mediterranean outflow at the traverse of Cadiz was 1 order of magnitude lower than

calculations for the Strait of Gibraltar. More studies on the carbon cycle during different seasons with similar scales are needed to understand the importance of the Gulf of Cadiz continental shelf in the global carbon cycle.

[43] **Acknowledgments.** We would like to thank the crew of the RV *Cornide de Saavedra* for their cooperation at sea and L. M. Laglera for his help with sample collection and alkalinity determination. Special thanks are given to M. J. Brogueira and G. Cabecadas who kindly provided the nutrient data, and also to C. Copin-Montégut and A. F. Ríos and two anonymous reviewers for their discussion points and constructive criticism, which has enabled us to improve this paper, and also to Heather Adams for proofreading our study. This research was funded by the European Commission, CANIGO Programme (contract MAS3 - CT96 - 0060).

References

- Ambar, I., A shallow core of Mediterranean water off western Portugal, *Deep Sea Res., Part A*, 30, 677–680, 1983.
- Ambar, I., and M. R. Howe, Observation of the Mediterranean outflow: I. Mixing in the Mediterranean outflow, *Deep Sea Res.*, 26, 535–554, 1979a.
- Ambar, I., and M. R. Howe, Observation of the Mediterranean outflow: II. The deep circulation in the vicinity of the Gulf of Cádiz, *Deep Sea Res.*, 26, 555–568, 1979b.
- Ambar, I., M. R. Howe, and M. I. Abdullan, A physical and chemical description of the Mediterranean outflow in the Gulf of Cádiz, *Dtsch. Hydrogr. Z.*, 29, 58–68, 1976.
- Arhan, M., A. C. Verdière, and L. Mémery, The eastern boundary of the subtropical North Atlantic, *J. Phys. Oceanogr.*, 24, 1295–1316, 1994.
- Bakker, D. C. E., H. J. W. De Baar, and P. J. De Wilde, Dissolved carbon dioxide in Dutch coastal waters, *Mar. Chem.*, 55, 247–263, 1996.
- Bakker, D. C. E., H. J. W. De Baar, and U. V. Bathmann, Changes in carbon dioxide in surface waters during spring in the Southern Ocean, *Deep Sea Res., Part II*, 44, 91–127, 1997.
- Bellerby, R. G. J., D. R. Turner, G. E. Millward, and P. J. Worsfold, Shipboard flow injection determination of sea water pH with spectrophotometric detection, *Anal. Chim. Acta*, 309, 259–270, 1995.
- Brewer, P. G., D. M. Glover, C. Goyet, and D. K. Shaver, The pH of North Atlantic Ocean, improvements to the global model for sound absorption in seawater, *J. Geophys. Res.*, 100, 8761–8776, 1995.
- Butler, J. H., C. M. Elkins, C. M. Bruson, K. B. Egan, T. M. Thompson, T. J. Conway, and B. D. Hall, Trace gases in and over the west Pacific and East Indian Oceans during the El Niño-Southern Oscillation event of 1987, *NOAA Data Rep. ERL-ARL-16*, 104 pp., Air Resour. Lab., Silver Spring, Md., 1988.
- Cano, N., Resultados de la campaña “Alborán-76,” *Bol. Inst. Esp. Oceanogr.*, 247, 3–50, 1978.
- Clayton, T. D., and R. H. Byrne, Spectrophotometric seawater pH measurements: Total hydrogen ion concentration scale calibration of m-cresol purple and at-sea results, *Deep Sea Res.*, 42, 411–429, 1993.
- Copin-Montégut, C., Alkalinity and carbon budgets in the Mediterranean Sea, *Global Biogeochem. Cycles*, 7(4), 915–925, 1993.
- Dafner, E. V., R. Sempéré, N. González, F. Gomez, and M. Goutx, Cross-slope variations of dissolved organic carbon in the Gulf of Cádiz, NE Atlantic Ocean (February 1998), *Mar. Ecol. Prog. Ser.*, 189, 301–306, 1999.
- Dafner, E. V., M. González-Dávila, J. M. Santana-Casiano, and R. Sempéré, Total organic and inorganic carbon exchange through the Strait of Gibraltar in September 1997, *Deep Sea Res., Part I*, 48, 1217–1235, 2001.
- DelValls, T. A., and A. G. Dickson, The pH buffers based on 2-amino-2-hydroxymethyl-1, 3-propanediol (“tris”) in synthetic sea water, *Deep Sea Res., Part I*, 45, 1541–1554, 1998.
- Department of Energy, Handbook of method for the analysis of the various parameters of the carbon-dioxide system in sea water, vers. 2, edited by A. G. Dickson and C. Goyet, *ORNL/CDIAC-74*, Dep. of Energy, Washington, D. C., 1994.
- Dickson, A. G., An exact definition of total alkalinity and a procedure for the estimation of alkalinity and total inorganic carbon from titration data, *Deep Sea Res.*, 28, 609–623, 1981.
- Dickson, A. G., and F. J. Millero, A comparison of the equilibrium constants for the dissociation of carbonic acid in seawater media, *Deep Sea Res., Part I*, 34, 1733–1743, 1987.
- Fraga, F., A. F. Ríos, F. F. Pérez, and F. G. Figueiras, Theoretical limits of oxygen:carbon and oxygen:nitrogen ratios during photosynthesis and mineralisation of the organic matter in the sea, *Sci. Mar.*, 62, 161–168, 1998.

- Gómez, F., F. Echevarría, C. M. García, L. Prieto, J. Ruiz, A. Reul, F. Jiménez-Gómez, and M. Varela, Microplankton distribution in the Strait of Gibraltar: Coupling between organisms and hydrodynamic structures, *J. Plankton Res.*, 22(4), 603–617, 2000.
- Hansen, H. P., and K. Grasshoff, Automated chemical analysis, in *Methods of Seawater Analysis*, edited by K. Grasshoff et al., pp 347–395, Verlag Chemie, Weinheim, Germany, 1983.
- Körtzinger, A., J. I. Hedges, and P. D. Quay, Redfield ratios revisited: Removing the biasing effect of anthropogenic CO₂, *Limnol. Oceanogr.*, 46, 964–970, 2001.
- Lee, K., F. J. Millero, and R. Wanninkhof, The carbon dioxide system in the Atlantic Ocean, *J. Geophys. Res.*, 102, 15,693–15,707, 1997.
- Lee, K., F. J. Millero, R. H. Byrne, R. A. Feely, and R. Wanninkhof, The recommended dissociation constants for carbonic acid in seawater, *Geophys. Res. Lett.*, 27, 229–232, 2000.
- Madelaine, F., Calculs dynamiques au large de la Peninsula Iberique, *Cah. Oceanogr.*, 19, 181–194, 1967.
- Millero, F. J., Thermodynamics of the carbon dioxide system in the oceans, *Geochim. Cosmochim. Acta*, 59, 661–677, 1995.
- Millero, F. J., E. A. Degler, D. W. O'Sullivan, C. Goyet, and G. Eiseheid, The carbon dioxide system in the Arabian Sea, *Deep Sea Res., Part II*, 45, 2225–2252, 1998.
- Minas, H. J., and M. Minas, Influence du détroit de Gibraltar sur la biogéochimie de la Méditerranée et du proche Atlantique, *Ann. Inst. Oceanogr.*, 69(1), 203–214, 1993.
- Minas, H. J., B. Coste, P. Le Corre, M. Minas, and P. Raimbault, Biological and geochemical signatures associated with the water circulation through the Strait of Gibraltar and in the Western Alboran Sea, *J. Geophys. Res.*, 96, 8755–8771, 1991.
- Mintrop, L. M., F. F. Pérez, M. González-Dávila, J. M. Santana-Casiano, and A. Körtzinger, Alkalinity determination by potentiometry: Intercalibration using three different methods, *Cienc. Mar.*, 26, 23–37, 2000.
- Ochoa, J., and N.A. Bray, Water mass exchange in the Gulf of Cádiz, *Deep Sea Res.*, 38, Suppl. 1, S465–S503, 1991.
- Packard, T. T., et al., Formation of the Alboran oxygen minimum zone, *Deep Sea Res.*, 35, 1111–1118, 1988.
- Parrilla, G., (Ed.), Mid-term scientific report, *CANIGO-MAST 3-CT 96-0060*, 321 pp., Inst. Esp. de Oceanogr., Madrid, 1998.
- Parsons, T. R., T. J. Takahashi, and B. Hargrave, *Biological Oceanographic Processes*, 332 pp., Pergamon Press, New York, 1977.
- Pérez, F. F., M. Estrada, and J. Salat, Sistema del carbónico, oxígeno y nutrientes en el Mediterráneo occidental, *Inv. Pesq.*, 50(3), 333–351, 1986.
- Pérez, F. F., A. F. Ríos, C. G. Castro, and F. Fraga, Mixing analysis of nutrients, oxygen and dissolved inorganic carbon in the upper and middle North Atlantic Ocean east of the Azores, *J. Mar. Syst.*, 16, 219–233, 1998.
- Pérez, F. F., M. Alvarez, and A. F. Ríos, Improvements on the back-calculation technique for estimating anthropogenic CO₂, *Deep Sea Res., Part I*, 49, 859–875, 2002.
- Price, J. F., M. O. Baringer, R. G. Lueck, G. C. Johnson, I. Ambar, G. Parrilla, A. Cantos, M. A. Kennely, and T. B. Sanford, Mediterranean outflow mixing and dynamics, *Science*, 259, 1277–1282, 1993.
- Rahmstorf, S., Influence of Mediterranean outflow on climate, *Eos Trans. AGU*, 79(24), 281–282, 1998.
- Ríos, A. F., T. R. Anderson, and F. F. Pérez, The carbonic system distribution and fluxes in the NE Atlantic during spring 1991, *Prog. Oceanogr.*, 35, 295–314, 1995.
- Ríos, A. F., F. Fraga, F. G. Figueiras, and F. F. Pérez, A modelling approach to the Redfield ratio deviations in the ocean, *Sci. Mar.*, 62, 169–176, 1998.
- Sabine, C. L., F. T. Mackenzie, C. Winn, and D. M. Karl, Geochemistry of carbon dioxide in seawater at the Hawaii Ocean Time series station, ALOHA, *Global Biogeochem. Cycles*, 9(4), 637–651, 1995.
- Santana-Casiano, J. M., M. González-Dávila, and L. Laglera, Carbon dioxide system in the Strait of Gibraltar, *Deep Sea Res., Part II*, 49, 4145–4161, 2002.
- Schneider, B., K. Kremling, and J. C. Duinker, CO₂ partial pressure in northeast Atlantic and adjacent shelf waters: Processes and seasonal variability, *J. Mar. Syst.*, 3, 453–463, 1992.
- Siegenthaler, U., and J. L. Sarmiento, Atmospheric carbon dioxide and the ocean, *Nature*, 365, 119–125, 1993.
- Takahashi, T., W. S. Broecker, and S. Langer, Redfield ratio based on chemical data from isopycnal surfaces, *J. Geophys. Res.*, 90, 6907–6924, 1985.
- Tans, P. P., I. Y. Fung, and T. Takahashi, Observational constraints on the global atmospheric CO₂ budget, *Science*, 247, 1431–1438, 1990.
- Tomczak, J. R., A multi-parameter extension of temperature/salinity diagram for the analysis of non-isopycnal mixing, *Prog. Oceanogr.*, 10, 147–171, 1981.
- Transient Tracers in the Oceans North Atlantic Study, Shipboard physical and chemical data report, 1 April–19 October 1981, Scripps Inst. of Oceanogr., Univ. of Calif., San Diego, Calif., 1981.
- United Nations Educational, Scientific, and Cultural Organization, Progress on Oceanographic Tables and Standards 1983–1986, *Tech. Pap. Mar. Sci.*, 50, 59 pp., 1986.
- Van Geen, A., P. Rosener, and E. Boyle, Entrainment of trace-metal-enriched Atlantic-shelf water in the inflow to the Mediterranean Sea, *Nature*, 331, 423–426, 1988.
- Van Geen, A., E. Boyle, and W. S. Moore, Trace metals enrichments in waters of Gulf of Cádiz, Spain, *Geochim. Cosmochim. Acta*, 55, 2173–2191, 1991.
- Wallace, D. W. R., Monitoring global ocean carbon inventories, *Background Rep. 5*, 54 pp., Tex. A&M Univ., College Station, Tex., 1995.
- Wanninkhof, R., Relationship between wind speed and gas exchange over the ocean, *J. Geophys. Res.*, 97, 7373–7383, 1992.
- Wanninkhof, R., and K. Thoning, Measurement of fugacity of CO₂ in surface water using continuous and discrete sampling methods, *Mar. Chem.*, 44, 189–204, 1993.
- Weiss, R. F., Carbon dioxide in water and seawater: The solubility of a non ideal gas, *Mar. Chem.*, 2, 203–215, 1974.
- World Ocean Circulation Experiment, *WOCE Operations Manual*, vol. 3, sect. 3.1, part 3.1.3, *WHP Operations and Methods*, rev. 1, Nov. 1994, Woods Hole, Mass., 1994.
- Zenk, W., Some current and temperature observations in the Mediterranean outflow west of Gibraltar, *Meteor. Forschungsergeb.*, A, 15, 20–48, 1975.

E. V. Dafner, Department of Oceanography, School of Ocean, Earth Sciences and Technology, University of Hawaii, Manoa, 1000 Pope Rd., Honolulu, HI 96822, USA. (evgeny@hawaii.edu)

M. González-Dávila and J. Magdalena Santana-Casiano, Chemistry Department, Las Palmas de Gran Canaria University, S-35017 Las Palmas, Gran Canaria, Spain. (mgonzalez@dqui.ulpgc.es; jmsantana@dqui.ulpgc.es)